THE JOURNAL OF BIOLOGICAL CHEMISTRY
Vol. 279, No. 46, Issue of November 12, pp. 47849–47855, 2004

*Printed in U.S.A.*

# Electrostatic Interaction between Redox Cofactors in Photosynthetic Reaction Centers*

Received for publication, August 4, 2004, and in revised form, August 27, 2004
Published, JBC Papers in Press, August 30, 2004, DOI 10.1074/jbc.M408888200

**Jean Alric‡§, Aude Cuni¶§, Hideaki Maki‖, Kenji V. P. Nagashima‖, André Verméglio**, and Fabrice Rappaport¶‡‡**

*From the ‡Laboratoire de Génétique et Biophysique des Plantes, UMR 6191 CNRS-CEA-Aix-Marseille II, 163 avenue de Luminy, Marseille 13288, France, ¶Institut de Biologie Physico-Chimique, CNRS UPR 1261, 13 rue P. et M. Curie, 75005 Paris, France, ‖Department of Biology, Tokyo Metropolitan University, Minamiohsawa 1-1, Hachioji, Tokyo 192-0397, Japan, and **CEA-Cadarache DSV-DEVM Laboratoire de Bioénergétique Cellulaire, UMR 6191 CNRS-CEA-Aix-Marseille II, F-13108 Saint Paul lez Durance Cedex, France*

**Intramolecular electron transfer within proteins is an essential process in bioenergetics. Redox cofactors are embedded in proteins, and this matrix strongly influences their redox potential. Several cofactors are usually found in these complexes, and they are structurally organized in a chain with distances between the electron donor and acceptor short enough to allow rapid electron tunneling. Among the different interactions that contribute to the determination of the redox potential of these cofactors, electrostatic interactions are important but restive to direct experimental characterization. The influence of interaction between cofactors is evidenced here experimentally by means of redox titrations and time-resolved spectroscopy in a chimeric bacterial reaction center (Maki, H., Matsuura, K., Shimada, K., and Nagashima, K. V. P. (2003) *J. Biol. Chem.* 278, 3921–3928) composed of the core subunits of *Rubrivivax gelatinosus* and the tetraheme cytochrome of *Blastochloris viridis*. The absorption spectra and orientations of the various cofactors of this chimeric reaction center are similar to those found in their respective native protein, indicating that their local environment is conserved. However, the redox potentials of both the primary electron donor and its closest heme are changed. The redox potential of the primary electron donor is downshifted in the chimeric reaction center when compared with the wild type, whereas, conversely, that of its closet heme is upshifted. We propose a model in which these reciprocal shifts in the midpoint potentials of two electron transfer partners are explained by an electrostatic interaction between them.**

Proteins exert a fine electrochemical tuning of the redox potential of the cofactors they bind in order to perform the various electron transfer reactions that are involved in biological processes. As a famous example, the redox potentials ($E_m$)[1] of *c*-type cytochromes are tuned by more than 500 mV (see Ref. 1 and references therein). The physicochemical basis of a such wide range of modulations has been rationalized by various authors who all agree that the protein medium has the unique property of providing a dielectric environment in which the redox cofactors are embedded with an intricate charge or dipole distribution (1–3). From a general standpoint, the free energy difference between the oxidized and reduced forms of any redox cofactor in a protein is the sum of several terms. Among these are $\Delta G_{conf}$ and $\Delta G_{el}$. $\Delta G_{conf}$ accounts for any conformational change that the change in the redox state of the cofactor may induce (including proton or ion binding or release). $\Delta G_{el}$ results from the electrostatic potential at the cofactors resulting from the individual charged groups and the permanent dipoles within the protein. Estimating the respective values of these different terms is a difficult task, yet their sum is readily accessible experimentally because it can be obtained by comparing the absolute values of the $E_m$ in solution and in the protein. The latter may be obtained by two different methods. The most commonly used one is equilibrium redox titration. The other relies on the determination, by a functional analysis, of the free energy change associated with an electron transfer reaction between two cofactors. Such a change in free energy is generally considered as equal to the difference in $E_m$s between the electron donor and acceptor. Thus, provided that one of these two redox potentials is known, the other one is readily inferred. However, these two methods sometimes yield different results and this has led to the distinction between "equilibrium redox potential" and "operating redox potential." These differences arise because the two methods do not probe the same state of the redox cofactors. Two types of phenomena may account for these differences. One comes from the distinct time domain involved in equilibrium redox titration and functional analysis. Whereas redox titrations require thermodynamic equilibrium between the sample and the solution poised at a given potential, the functional analysis allows one to probe transient states whose free energy may differ significantly from that of the equilibrated states. Indeed, in response to the change in the redox state of a given cofactor, the protein environment may undergo energetic relaxation (such as proton transfer, conformational changes), which may be slower than the lifetime of the transient oxidized (or reduced) cofactor. Armstrong *et al.* (4) have nicely illustrated this point with the "fast-scan electrovoltammetric" technique. Other examples are found in photosynthetic reaction centers (RC) (for example, see Refs. 5 and 6). An alternative but non-exclusive explanation of the different $E_m$s yielded by redox titration and functional analysis relies on the fact that most of the membrane proteins involved in electron transfer reactions bind several cofactors, which are usually located at less than 15 Å, one from the other.

* The costs of publication of this article were defrayed in part by the payment of page charges. This article must therefore be hereby marked "*advertisement*" in accordance with 18 U.S.C. Section 1734 solely to indicate this fact.

§ Both authors contributed equally to the work.

‡‡ To whom correspondence should be addressed. Tel.: 33-1-58-41-50-59; Fax: 33-1-58-41-50-22; E-mail: Fabrice.Rappaport@ibpc.fr.

[1] The abbreviations used are: $E_m$, midpoint redox potential; $E_h$, ambient redox potential; P, primary electron donor; RC, reaction center; WT, wild type; MOPS, 4-morpholinepropanesulfonic acid; $g_2$, *2* tensor component.

Such short distances may result in significant electrostatic interactions among the different cofactors. Thus, for a given cofactor, $\Delta G_{el}$ includes the electrostatic contributions of the nearby electron carriers. Such a contribution has been nicely illustrated in the case of the tetraheme cytochrome of *Blastochloris* (formerly *Rhodopseudomonas*) *viridis* (7, 8). However, it is noteworthy that throughout a redox titration, all of the cofactors undergo an identical charge change in terms of sign (*i.e.* all are either reduced or oxidized), whereas in an electron transfer chain, two nearby cofactors involved in an electron transfer reaction will undergo charge changes of opposite sign (one will be oxidized at the expense of the other). Consequently, if the electrostatic interaction between the two is significant, the difference between their equilibrium $E_m$s will be greater than the free energy change associated with the electron transfer between them. In this paper, we illustrated the importance of such electrostatic interactions in electron transfer chains. Although electron transfer chains embedded in a single protein are found in many biological pathways, the photosynthetic chains are ideally suited for such studies. Indeed, not only do they allow redox titration of the various redox cofactors, but also the kinetics of electron transfer reaction may be characterized with an unequalled time resolution. In particular, the bacterial photosynthetic RC of *B. viridis* and its associated tetraheme cytochrome have been intensively studied. Its three-dimensional structure has been solved (9), and the spectroscopic or redox properties of the various cofactors are known (see Ref. 10 for a review). Further, the different electron transfer steps have been characterized (11). In membrane fragments as well as purified RC of *B. viridis*, the reduction of the oxidized primary electron donor $P^+$ by the closest heme, $c_{559}$, is multiphasic (12). Interestingly, this feature has been interpreted along the lines of either of the two phenomena that has just been described, a conformational heterogeneity yielding a distribution of substates (11) or a low equilibrium constant of this electron transfer reaction (13). To reconcile this latter hypothesis with the equilibrium constant of ~100 expected from the difference in midpoint potentials of the $P^+/P$ and $c_{559}{}^+/c_{559}$, Baymann and Rappaport (13) proposed that an electrostatic interaction between P and its closest heme raises the redox potential of the $P^+/P$ couple. As discussed below, the present results support this hypothesis.

From an experimental standpoint, *B. viridis* has the drawback of being unable to grow heterotrophically, making the mutagenesis approach uncertain despite a few successful attempts. Recently, Maki *et al.* (14) succeeded in transferring the membrane bound cytochrome of *B. viridis* to another bacterium, *Rubrivivax gelatinosus*, in which mutagenesis strategy may be planned (15, 16).

In this paper, we further investigated this chimeric RC (hereafter named VC-F) and show that most of the various cofactors at the donor side of this RC show absorption spectra and relative orientations similar to those found in the respective native RCs, indicating that the backbone structure of the protein as well as the interactions between the hemes and the side chains are conserved (Fig. 1). These findings make the chimeric RC suited for the direct characterization of electrostatic interactions between cofactors by the mean of equilibrium redox titration. Indeed, in this RC, two cofactors (the primary electron donor (P) and the closest heme $c_{559}$) are expected to have redox potentials differing by less than 50 mV (see Fig. 1). Such a case allows the direct observation of a putative electrostatic interaction, because it should manifest itself by a deviation to a one-electron Nernst curve. This contrasts with the case where the two interacting redox centers have strongly different midpoint potentials (as in the *B. viridis* case, for example) for they are then expected to titrate in well separated redox potential ranges and thus yield titration curves that follow the classical Nernst equation. Accordingly, we found that the redox titration of the primary donor ($P/P^+$) of the chimeric RC displayed a deviation to a one-electron Nernst curve. The redox potential of the primary donor was downshifted by 50 mV in the chimera with respect to the WT *R. gelatinosus* strain. Interestingly, the redox potential of the closest heme (the $c_{559}$ heme) underwent a converse upshift of similar amplitude. These data prove that electrostatic interactions between cofactors in proteins modulate their redox potentials.

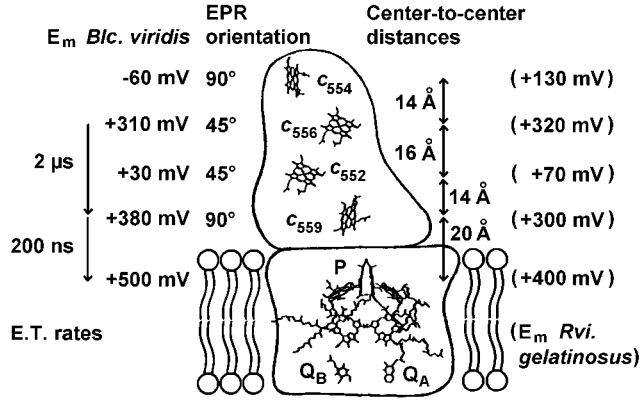


FIG. 1. **Schematic view of the bacterial reaction center of *B. viridis* and *R. gelatinosus*.** $E_m$ values are indicated for each species (see Refs. 10, 13, 25, and 38 for *B. viridis* (*Blc. viridis*) and Refs. 10 and 22 for *R. gelatinosus* (*Rvi. gelatinosus*). Electron transfer (*E.T.*) rates between cofactors (12, 13) as well as orientation of the hemes relative to the membrane plane (determined by EPR spectroscopy) (24) are indicated for *B. viridis*.

## EXPERIMENTAL PROCEDURES

Interspecific replacement of the gene coding for the RC-bound cytochrome subunit in *R. gelatinosus* used to produce VC-F mutant is described by Maki *et al.* (14). The site-directed substitution by a two-step PCR method of Arg-204 for a Leu in the cytochrome subunit of the VC-F strain is described by Nagashima *et al.* (17).

Cells of the VC-F mutant of *R. gelatinosus* were grown for 24 h in the light and in anaerobic conditions in Hutner medium with 50 $\mu g \cdot ml^{-1}$ kanamycin and 20 $\mu g \cdot ml^{-1}$ ampicillin. For membrane preparations, cells were harvested by centrifugation at 4000 × *g* for 10 min, resuspended in 20 mM Tris-HCl (pH 7), and disrupted by a French press at 50 megapascals. The remaining intact cells were separated from the membrane supernatant by centrifugation at 10,000 × *g* for 10 min. The membrane fragments then were collected after centrifugation at 250,000 × *g* for 90 min and resuspended in 20 mM Tris-HCl, 100 mM KCl (pH 7), for equilibrium redox titrations.

*EPR Spectroscopy*—Membrane fragments were resuspended in 20 mM MOPS (pH 7) and oxidized by the addition of 2 mM potassium ferricyanide. The membranes were then washed free from ferricyanide by renewed pelleting and resuspension in 20 mM MOPS (pH 7). Electron paramagnetic response spectra were taken at 15 K using a Bruker ER 300 X-band spectrometer equipped with an Oxford Instruments helium cryostat and temperature-control system. The instrument settings were as follows: microwave power, 6.7 milliwatts; microwave frequency, 9.43 GHz; and modulation amplitude, 2.5 millitesla. Angular dependence of EPR signals was investigated on oriented membrane multilayer obtained by drying the membrane fragments onto Mylar sheets (18).

Redox titrations were performed as described previously (13, 19) in an electrochemical cell (100-$\mu$m optical path length) with three electrodes: a platinum electrode; a gold grid (InterNet Inc.) modified by PATS (2-pyridinecarboxaldehyde thiosemicarbazone, Sigma) to avoid irreversible adsorption of the proteins onto the gold grid; and an Ag/AgCl reference electrode in 3 M KCl. The redox mediators were used at 20 $\mu$M each: 1,4-benzoquinone ($E_m$ = +280 mV); 1,1-dimethyl ferrocene ($E_m$ = +340 mV); ferrocene ($E_m$ = +420 mV); and monocarboxylic acid ferrocene ($E_m$ = +530 mV).

The optical spectroscopic measurements were performed on two different laboratory-built absorption spectrophotometers: a Xenon flashlamp microsecond time resolution one (20) used for the titration of

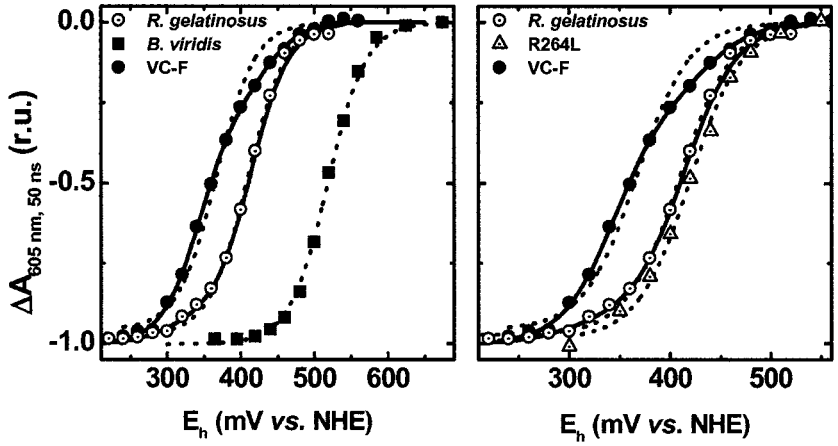


FIG. 2. **Flash-induced equilibrium redox titration of the primary electron donor P.** Flash-induced electrochemical redox titrations were performed at thermodynamic equilibrium by monitoring the light-induced absorbance changes at 605 nm (*i.e.* in the $Q_x$ absorption band of bacteriochlorophylls), 50 ns after the saturating flash. The negative absorbance change at this wavelength is proportional to the amount of P that can be photo-oxidized and thus yields the amount of reduced P in the dark. Experimental data were fitted with a one-electron Nernst curve (*dashed lines*) and with Equation 12 (*solid lines*). *Left panel*, *B. viridis* (*closed squares*) together with *R. gelatinosus* WT and chimeric RC (*open* and *closed circles*, respectively). *Right panel*, *R. gelatinosus* WT (*open circles*), native chimeric RC (*closed circles*), and R264L mutant of the chimeric RC (*triangles*). *r.u.*, relative units; *Blc. viridis*, *B. viridis*; *Rvi. gelatinosus*, *R. gelatinosus*; NHE, normal hydrogen electrode.

the cytochromes in the α-band and a Nd:YAG-pulsed laser nanosecond time resolution one (21) used for the kinetic experiments and the flash-induced titration of the primary electron donor.

## RESULTS

*Redox Characteristics of the $P^+$/P Couple in the WT and Chimeric RCs*—The primary electron donor P was titrated in membrane fragments purified from *R. gelatinosus* and *B. viridis* WT strains and the chimeric VC-F strain (Fig. 2, *left panel*) by measuring the flash-induced absorption changes at 605 nm, 50 ns after the actinic flash. Both the oxidative or reducing waves yielded similar results, indicating that thermodynamic equilibrium was reached during the titration (data not shown). The titration curve in *B. viridis* could be satisfyingly fitted with a Nernst curve with $E_m$ = +500 mV. The $P^+$/P couple in *R. gelatinosus* titrates with an $E_m$ of ~+400 mV, consistent with previous findings (22), but, interestingly, the titration curve showed a slight deviation to a one-electron Nernst equation (*dotted line*). In the VC-F-chimeric RC, the results were significantly different from that in *R. gelatinosus* WT. (i) The deviation to the one-electron Nernst equation (*dotted line*) was more pronounced. (ii) The overall midpoint potential was lower by ~50 mV.

Several non-exclusive hypotheses may account for such a difference. The first one relies on a strong heterogeneity among the RCs. As a possible reason for such heterogeneity, one may consider that the tetraheme subunit is lost in a fraction of RCs during the preparation of the membrane fragments. To test this hypothesis, we measured (Fig. 3) the amount of long-lived $P^+$ under conditions where only the $c_{556}$ and $c_{559}$ hemes were reduced in the dark (Fig. 3, *squares*) and under conditions where the high and low potential hemes were reduced in the dark (Fig. 3, *triangles*). Whereas in the former case ~50% $P^+$ was still present 200 μs after the flash, this fraction of long-lived $P^+$ was only 3% when the low potential hemes were reduced. Under these latter conditions, the free energy change associated with $P^+$ reduction is expected to be large because of the low midpoint potentials of the electron donor (see Fig. 1). Thus, after this equilibrium is reached (*i.e.* in the hundreds of a microsecond time range, see Fig. 1), the amount of $P^+$ remaining should be too low to be detectable. Conversely, in the eventual RCs devoid of the tetraheme subunit, $P^+$ is expected to decay via charge recombination, *i.e.* in the tens of a millisecond time range (23). Thus, the amount of $P^+$ still detectable at 200 μs after the actinic flash can be taken as an indication of the amount of RCs with no tetraheme subunit. Moreover, the absorption changes measured 200 μs after the flash were indicative of the flash-induced oxidation of a low potential heme (data not shown). We take these results as evidence that most of the RCs (97%) have a bound and functional cytochrome subunit.

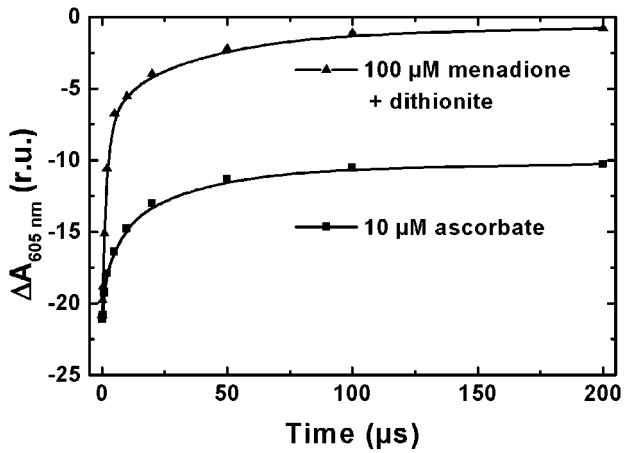


FIG. 3. **Flash-induced kinetics of $P^+$ reduction by the RC-bound cytochrome under moderately oxidizing potential ($E_h$ ~+200 mV; ascorbate, *squares*) or low-potential conditions ($E_h$ ~ 0 mV; menadione + dithionite, *triangles*).** The redox potential of membrane fragments of the VC-F strain was poised by the addition of ascorbate or menadione and sodium dithionite and monitored by a combined reference electrode. *r.u.*, relative units.

Another possible explanation of the different titration curves in the VC-F and WT RCs is a structural modification of the protein matrix around the bacteriochlorophyll dimer resulting from the chimeric association with the *B. viridis* cytochrome subunit. We consider this hypothesis as unlikely as well, because the absorption changes associated with the formation of the $P^+$ state in the VC-F mutant were similar to those observed with the WT *R. gelatinosus* RC (Fig. 4*A*). Further, EPR measurements performed on VC-F-oriented membrane multilayer dried on Mylar sheets showed an angle dependence of the $g_z$ signal of the hemes identical to that obtained for *B. viridis*. Nitschke and Rutherford (24) assigned the EPR $g_z$ signals of each of the four hemes in the *B. viridis* cytochrome on the basis of their respective $E_m$. They ascribed the *g*-value of 3.09 to the highest potential $c_{559}$ heme and *g*-values comprised between

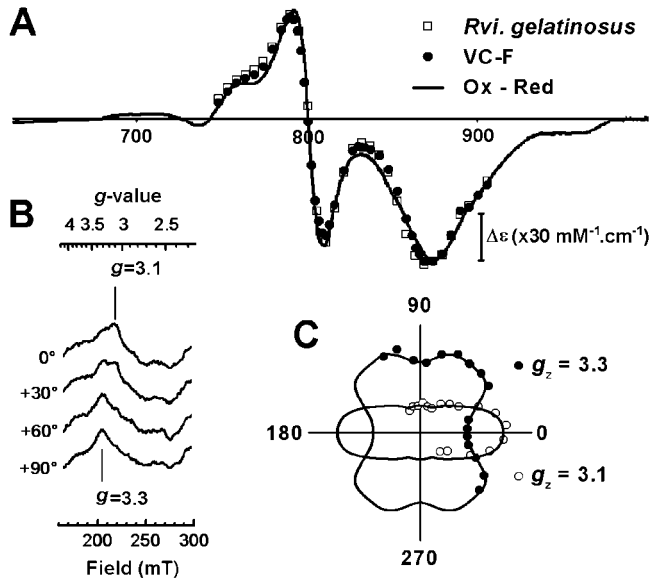


FIG. 4. **Spectroscopic characterization of the chimeric reaction center.** *A*, difference absorption spectra of the primary electron donor P recorded in the $Q_y$ band of the bacteriochlorophyll special pair: 1) the flash-induced oxidation of partially oxidized membranes of *R. gelatinosus* (*open squares*) and VC-F (*closed circles*) 100 ms after the flash and 2) oxidized minus-reduced purified VC-F RCs (*solid line*). *B*, EPR spectra recorded on oriented membrane multilayers of VC-F dried on Mylar sheets. *C*, orientation dependence of the EPR signal amplitudes from *panel B*. *Rvi. gelatinosus*, *R. gelatinosus*.

3.29 and 3.32 to the other hemes. The global binding of the *B. viridis* cytochrome onto the RC of *R. gelatinosus* was investigated in the same way. Oriented multilayers of VC-F membrane fragments exhibited peaks at *g*-values of 3.1 and 3.3 with orientation-dependent intensities (Fig. 4*B*). Polar plots of EPR signal amplitudes allowed one to orient the $g_z$ of 3.1 along the 0° axis, whereas the maximum of the $g_z = 3.3$ line was found at 45° (Fig. 4*C*). Since the $g_z$ vector of a heme is perpendicular to the porphyrin ring, we concluded that the highest potential heme $c_{559}$ was almost perpendicular (90°) to the membrane plane, similar to *B. viridis* (compare Fig. 4*C* with Fig. 7 in Ref. 24). Moreover, the absorption spectra of the four hemes bound to the tetraheme subunit are conserved in the chimeric RC with respect to the WT *B. viridis* RC (see Fig. 5*A* for a comparison of absorption changes associated with the oxidation of the $c_{556}$ and $c_{559}$ hemes in both strains). Furthermore, the $E_m$s of the three lower potential hemes embedded in the cytochrome subunit are remarkably conserved when compared with those found in *B. viridis* (14). Based on the sensitivity of both the spectroscopic and redox properties of a redox cofactor to any significant alteration of its protein environment, we take these results as a strong indication in favor of a conserved structure.

As a third hypothesis, which would account for the singular titration curve of the $P^+$/P couple in the VC-F strain, we would now like to consider the existence of a significant electrostatic interaction between the bacteriochlorophyll dimer and its nearest redox-active neighbor, the $c_{559}$ heme. Such an interaction between two close redox cofactors implies that the $E_m$ of either one of the two cofactors depends on the redox state of its neighbor. In the present framework, one should thus consider the following schemes as shown in Equations 1–5,[2]

$$\mathrm{P}c \overset{E_{\mathrm{P}(c)}}{\longleftrightarrow} \mathrm{P}^+ c + \mathrm{e}^- \quad \text{(Eq. 1)}$$

$$\mathrm{P}c^+ \overset{E_{\mathrm{P}(c^+)}}{\longleftrightarrow} \mathrm{P}^+ c^+ + \mathrm{e}^- \quad \text{(Eq. 2)}$$

$$\mathrm{P}c \overset{E_{c(\mathrm{P})}}{\longleftrightarrow} \mathrm{P}c^+ + \mathrm{e}^- \quad \text{(Eq. 3)}$$

$$\mathrm{P}^+ c \overset{E_{c(\mathrm{P}^+)}}{\longleftrightarrow} \mathrm{P}^+ c^+ + \mathrm{e}^- \quad \text{(Eq. 4)}$$

$$\text{with} \begin{cases} E_{\mathrm{P}(c^+)} = E_{\mathrm{P}(c)} + \Delta\psi \\ E_{c(\mathrm{P}^+)} = E_{c(\mathrm{P})} + \Delta\psi \end{cases} \quad \text{(Eq. 5)}$$

where $E_{\mathrm{P}(c^+)}$ and $E_{\mathrm{P}(c)}$ are the $E_m$ values of the $P^+$/P couple in the presence of the oxidized and reduced cytochromes, respectively, $\Delta\Psi$ is the electrostatic interaction between both cofactors, and $E_{c(\mathrm{P}^+)}$ and $E_{c(\mathrm{P})}$ are the $E_m$ values of the cytochrome in presence of $P^+$ and P, respectively. The equation used to fit the titration curve is then derived from both following points. 1) The total amount of oxidized $P^+$ or of reduced P can be written as shown in Equations 6 and 7.

$$[\mathrm{P}^+] = [\mathrm{P}^+c^+] + [\mathrm{P}^+c] \quad \text{(Eq. 6)}$$

$$[\mathrm{P}] = [\mathrm{P}c^+] + [\mathrm{P}c] \quad \text{(Eq. 7)}$$

2) Applying the Nernst equation at a given ambient potential ($E_h$) to the four electron transfer reactions just described yields Equations 8–11.

$$\frac{[\mathrm{P}^+c]}{[\mathrm{P}c]} = 10^{\frac{E_h - E_{\mathrm{P}(c)}}{60}} \quad \text{(Eq. 8)}$$

$$\frac{[\mathrm{P}^+c^+]}{[\mathrm{P}c^+]} = 10^{\frac{E_h - E_{\mathrm{P}(c^+)}}{60}} = 10^{\frac{E_h - E_{\mathrm{P}(c)} - \Delta\psi}{60}} \quad \text{(Eq. 9)}$$

$$\frac{[\mathrm{P}c^+]}{[\mathrm{P}c]} = 10^{\frac{E_h - E_{c(\mathrm{P})}}{60}} \quad \text{(Eq. 10)}$$

$$\frac{[\mathrm{P}^+c^+]}{[\mathrm{P}^+c]} = 10^{\frac{E_h - E_{c(\mathrm{P}^+)}}{60}} = 10^{\frac{E_h - E_{c(\mathrm{P})} - \Delta\psi}{60}} \quad \text{(Eq. 11)}$$

Incorporating Equations 8–11 into Equations 6 and 7 at a given $E_h$, the fraction of P in the oxidized state, irrespective of the redox state of the cytochrome is shown in Equation 12.

$$\frac{[\mathrm{P}^+]}{[\mathrm{P}^+] + [\mathrm{P}]} = \frac{10^{\frac{E_h - E_{\mathrm{P}(c)}}{60}} + 10^{\frac{2E_h - E_{c(\mathrm{P})} - E_{\mathrm{P}(c)} - \Delta\psi}{60}}}{1 + 10^{\frac{E_h - E_{\mathrm{P}(c)}}{60}} + 10^{\frac{E_h - E_{c(\mathrm{P})}}{60}} + 10^{\frac{2E_h - E_{c(\mathrm{P})} - E_{\mathrm{P}(c)} - \Delta\psi}{60}}} \quad \text{(Eq. 12)}$$

This equation allows one to distinguish several cases, each of the two extreme ones where $E_{\mathrm{P}(c)} \ll E_{c(\mathrm{P})}$ or $E_{c(\mathrm{P})} \ll E_{\mathrm{P}(c^+)}$ yields a redox titration, which follows a one-electron Nernst curve (with $E_m = E_{\mathrm{P}(c)}$ and $E_m = E_{\mathrm{P}(c)} + \Delta\Psi$, respectively). This reflects the fact that the redox changes of each cofactor occur in well separated redox potential ranges; thus, they do not interfere. A third and experimentally more interesting case arises when $E_{\mathrm{P}(c)} \approx E_{c(\mathrm{P})}$ or $E_{c(\mathrm{P})} \approx E_{\mathrm{P}(c^+)}$, because according to the above equation, the titration curve should be markedly different from a classical Nernst curve. This latter case applies to the VC-F strain. The data presented in Fig. 2 could be satisfyingly fitted to Equation 12 (Fig. 2, *solid lines*) with $E_{c(\mathrm{P})}$, $E_{\mathrm{P}(c)}$, and $\Delta\Psi$ as varying parameters. In the VC-F strain, the best-fit parameters were: $E_{c(\mathrm{P})} = +380$ mV; $E_{\mathrm{P}(c)} = +350$ mV; and $\Delta\Psi = +50$ mV. In the *R. gelatinosus* RC, the fit to Equation 12 yielded $E_{c(\mathrm{P})} = +300$ mV, $E_{\mathrm{P}(c)} = +350$ mV, and $\Delta\Psi = +50$ mV. In *B. viridis*, because the $E_m$s of the two interacting cofactors

[2] The reduced and oxidized states of the cytochrome are noted as *c* and $c^+$, respectively, for the sake of clarity. It does not mean that the absolute charge of the reduced cytochrome is null or that it is equal to one for the oxidized state. Yet, the change in charge resulting from the oxidation is equal to one electron.

belong to more distinct redox potential regions, the deviation to a one-electron Nernst curve was, as expected, less pronounced. The data could be satisfyingly fitted either with a one-electron Nernst curve with $E_P = +500$ mV or, according to Equation 12, with $E_{c(P)} = +380$ mV, $E_{P(c)} = +450$ mV, and $\Delta\Psi = +50$ mV. It is noteworthy that the values found for the $E_m$ of the $P^+/P$ couple as well as for $\Delta\Psi$ were similar in the chimeric and "parent" RC from *R. gelatinosus*. Yet, one could argue that the value found here for the $E_m$ of the $P^+/P$ couple in *R. gelatinosus* WT is 50 mV smaller than the previously reported one of 400 mV. This was not unexpected, because in the WT, the $E_m$ of the closest heme to P is significantly lower than that of the $P^+/P$ couple so that the respective oxidation (or reduction) of the two cofactors occurs in distinct redox potential domains. Consequently, the most significant fraction of P should be oxidized in the presence of the oxidized cytochrome and the titration curve should yield, as a first approximation, a $E_m$ of $E_{P(c)} + \Delta\Psi = 350 + 50 = +400$ mV, in good agreement with previous reports (22).

To further test this interpretation, we have measured the equilibrium redox titration of the $P^+/P$ couple in a site-directed mutant of the VC-F strain in which the $E_m$ of the $c_{559}$ heme is expected to be decreased, thereby increasing the gap between the $E_m$s of P and its closest heme. According to the calculation of Gunner and Honig (7), the presence of a positively charged arginine residue (Arg-264) in the vicinity of the $c_{559}$ heme of the *B. viridis* cytochrome subunit contributes to raise the midpoint potential of this redox center. This finding was confirmed by Chen *et al.* (26) who substituted, by site-directed mutagenesis, this residue for a lysine and found a downshifted $E_m$ for the $c_{559}$ by ~110 mV. We have also targeted this Arg and substituted it for a Leu in the gene coding for the tetraheme subunit in the VC-F strain (17). Consistent with the previous findings from Chen *et al.* (26), the $E_m$ of the $c_{559}$ heme in this mutant (R264L) was decreased to 130 mV (17) but the downshift was significantly larger, as expected from the less conservative mutation of the Arg residue into Leu rather than Lys.

Fig. 2 (*right panel*) shows a comparison of the equilibrium redox titration curve of P in the *R. gelatinosus*, VC-F WT, and R264L mutant strain (*open circles*, *solid circles*, and *triangles*, respectively). In line with the expectation that can be drawn from Equation 12, the apparent midpoint potential of P was upshifted in the R264L mutant with respect to the native VC-F RC and no significant deviation to a one-electron Nernst curve was observed. This result is fully consistent with the present model, according to which the deviation to a one-electron Nernst that witnesses the electrostatic interaction between two close redox centers becomes less prominent when increasing the difference between the $E_m$s of the two centers.

As a further support to our model, the $E_m$s of the hemes that were found to interact electrostatically with P when fitting the data with Equation 12 (+300 mV for *R. gelatinosus* WT and +380 mV for the VC-F strain) are consistent with the figures found in the literature for the closest hemes in the *R. gelatinosus* or *B. viridis* cytochrome subunit, respectively (see Fig. 1 for the data on the redox centers in the RC of these two species). Thus, we propose that the peculiar redox titration curve observed for the $P^+/P$ couple reflects a significant electrostatic interaction between P and the $c_{559}$ heme. One also expects the redox titration of the $c_{559}{}^+/c_{559}$ couple to be reciprocally affected by this interaction. To test this hypothesis, we performed the dark equilibrium titrations of both $c_{559}$ and $c_{556}$ hemes in *B. viridis* and VC-F RCs.

*Redox Characteristics of the Exogenous Cytochrome*—Absorbance changes were monitored in the $\alpha$-band region of the cytochromes (Fig. 5). The spectra in *panel A* show the characteristic features of the oxidation spectra of the $c_{556}$ and $c_{559}$ hemes, respectively (11, 25). They were found similar in the VC-F and *B. viridis* cases. In both cases, the titration curves of the $c_{556}$ and $c_{559}$ hemes were derived from the spectra at different $E_h$s for the $c_{556}$ by taking the difference between 556 and 562 nm, which cancels the $c_{559}$ contribution (Fig. 5*B*), and for the $c_{559}$ by taking the difference between 558 and 552 nm to cancel the contribution of $c_{556}$ (Fig. 5*C*). The titration curve of the $c_{556}$ heme was satisfyingly fitted by a one-electron Nernst equation and a $E_m$ of +310 mV in both the chimeric VC-F and WT *B. viridis* case, in agreement with previous reports for the *B. viridis* cytochrome subunit (11, 25). But the $E_m$ of the $c_{559}$ heme was 430 mV in the VC-F RC to be compared with the +380 mV found with *B. viridis* RC (this latter value being similar to previous findings) (13, 25). This 50-mV upshift matches our expectations nicely, because in the case of the VC-F strain, the $E_m$ of the $P^+/P$ couple was found lower than that of the $c_{559}$ heme. Thus, the majority of this heme should be oxidized (or reduced) in the presence of the oxidized form of P. Its apparent $E_m$ is thus expected to be: $E_{c(P)} + \Delta\Psi = 380 + 50 = +430$ mV, in agreement with the results shown in Fig. 2. However, we note that the titration curve of $c_{559}$ does not display a similar deviation to a one-electron Nernst curve as observed in the $P^+/P$ titration curve. This possibly arises from the difficulty to accurately cancel the contribution of the $c_{556}$ heme in the titration curve of the $c_{559}$ heme.

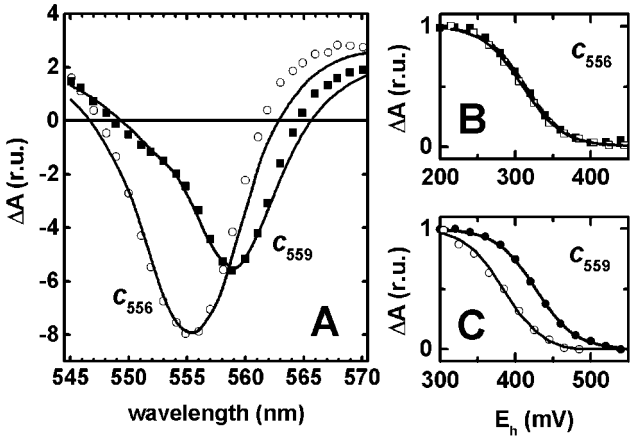


FIG. 5. **Dark equilibrium redox titration of the high potential hemes of VC-F and *B. viridis* RC.** The absorbance changes were recorded in the $\alpha$-band of the cytochromes. *Panel A*, difference absorption spectra of $c_{556}$ and $c_{559}$ oxidation with VC-F and *B. viridis* membrane fragments (*symbols* and *lines*, respectively). The $c_{556}$ and $c_{559}$ oxidation spectra were obtained by taking the difference between the spectra measured at +320 and +240 mV and measured at +500 and +400 mV, respectively. *Panel B*, titration curve of $c_{556}$ heme at 556 − 562 nm with VC-F (*solid symbols*) and *B. viridis* (*open symbols*) membrane fragments. *Panel C*, titration curve of $c_{559}$ heme at 558 − 552 nm VC-F (*solid symbols*) and *B. viridis* (*open symbols*) membrane fragments. *r.u.*, relative units.

*Kinetic Analysis of the Electron Transfer Reactions*—From the redox titration, we came to the conclusion that, under conditions where only the low potential hemes are oxidized, the redox potentials of the $P^+/P$, $c_{559}{}^+/c_{559}$, and $c_{556}{}^+/c_{556}$ are +350, +380, and +310 mV, respectively. Consequently, the reduction of $P^+$ by the $c_{559}$ heme is expected to be slightly uphill in energy and the oxidation of the $c_{556}$ heme by $P^+$ is expected to be only weakly downhill. These two features may be addressed by studying the flash-induced absorption changes. Indeed, a single turnover flash given to a dark-adapted sample results in the injection of a single oxidizing equivalent into the system and the time-dependent distribution of this charge among the various redox centers is expected to depend on their respective midpoint potential.

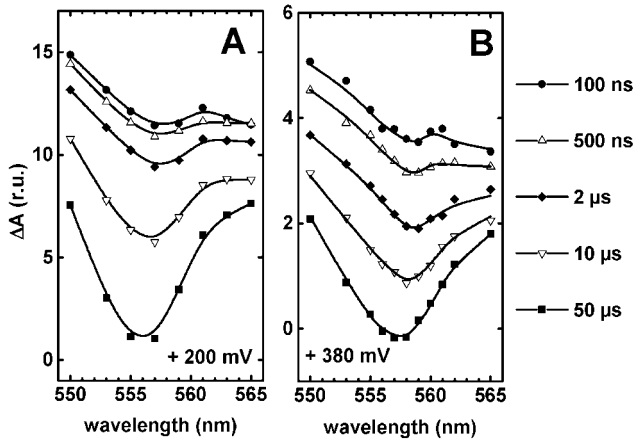


FIG. 6. **Time-resolved spectra of the flash-induced absorbance changes in the α-band of the cytochromes with VC-F membrane fragments.** The redox potential was poised at +200 and +380 mV (*left* and *right panel*, respectively). The experimental data (*symbols*) were fitted with a biexponential model, and the computed values are represented as *solid lines* (see "Results" for the amplitudes of the phases optimized by the global fit analysis). *r.u.*, relative units.

We first studied electron transfer reactions with membrane fragments poised at + 200 mV (Fig. 6*A*). Under such conditions, both $c_{556}$ and $c_{559}$ hemes are reduced before the flash. Whereas in *B. viridis* the reduction of $P^+$ occurs in the submicrosecond time range (11, 25), most of this reaction occurred in the chimeric RC with a half-time of 14 μs. The $c_{556}$ heme oxidation occurred concomitantly ($t_{1/2}$ ~12 μs), whereas the transient oxidation of the $c_{559}$ was hardly detectable.

To check the involvement of the $c_{559}$ in the oxidation of the $c_{556}$ heme by $P^+$, we measured the kinetics of absorption changes poising the redox potential at +380 mV (Fig. 6*B*). Under these conditions, because of their respective $E_m$s, a significant fraction of RCs should be in the $Pc_{559}/c_{556}^+$ state (~32%) before the actinic flash. In those RCs, the electron transfer step between $P^+$ and the $c_{559}$ heme should be clearly detectable. At 100 and 200 ns, the broad absorption increase reflects the photo-oxidation of P (for review see Ref. 13). In the 500-ns to 5-μs time range, a trough is observed with a minimum at 559 nm, suggesting the oxidation of the $c_{559}$ heme by the $P^+$. From 10 to 50 μs, the trough shifts to a lower wavelength, consistent with interheme $c_{556}/c_{559}$ electron transfer. The kinetics monitored at various wavelengths was globally fitted with two exponentials. The half-times of the fast and slow phases were found to be 700 ns and 11 μs, respectively.

One expectation that ensues from the redox titration is that the oxidation of the $c_{559}$ by $P^+$ should be energetically uphill. This prediction is supported by the present data. The fact that the $c_{559}$ oxidation step cannot be easily discriminated from the $c_{556}$ oxidation step suggests that the fraction of centers in the $Pc_{559}^+$ state in equilibrium with the $P^+c_{559}$ state is small. In the likely kinetic scheme describing the overall electron transfer reaction between $P^+$ and the $c_{556}$ heme, one can consider a two-step process where $k_1$, $k_{-1}$, $k_2$, and $k_{-2}$ are the forward and backward absolute rate constants of steps 1 and 2, respectively, as shown in Reaction 1.

$$(P^+, c_{559}, c_{556}) \underset{k_{-1}}{\overset{k_1}{\longleftrightarrow}} (P, c_{559}^+, c_{556}) \underset{k_{-2}}{\overset{k_2}{\longleftrightarrow}} (P, c_{559}, c_{556}^+)$$

REACTION 1

According to the $E_m$ of the three redox cofactors, the first step is energetically uphill and the second one is downhill. In addition, as in the case of *B. viridis*, if $k_2 < k_1$ (see Fig. 1), one expects the transiently formed $Pc_{559}^+/c_{556}$ to be hardly detectable. Interestingly, decreasing the relative amplitude of the second step by increasing the redox poise to oxidize the $c_{556}$ heme, for example, should enhance the relative amplitude of the first step, facilitating its detection in good agreement with the present data.

The unusually slow oxidation of the $c_{556}$ heme found in the VC-F RC with respect to the parents RC also supports the occurrence of an uphill step in the overall electron transfer from the $c_{556}$ to $P^+$ via the $c_{559}$ heme. In *B. viridis*, the apparent rate of the oxidation of the $c_{556}$ heme is ~$2.7 \times 10^5$ $s^{-1}$ (11, 13) to be compared with the $6.3 \times 10^4$ $s^{-1}$ value found in the chimeric RC. As a first approximation, the apparent rate of oxidation of the $c_{556}$ heme is, according to the above scheme, $k_{app} = k_2/(1 + k_{-1}/k_1)$. Assuming that the absolute rate of electron transfer between the two hemes ($k_2$) is unchanged in the chimera relative to *B. viridis* (an assumption that is supported by the above conclusion on the structural close similarities between both RCs) and taking $k_{-1}/k_1$ to $10^{30/60} = 3.2$ (corresponding to the $\Delta E_m$ between P and $c_{559}$ of −30 mV found here), one expects the apparent $c_{556}$ oxidation rate to be $k_{app} = 6.4 \times 10^4$ $s^{-1}$, in agreement with the value of $6.3 \times 10^4$ $s^{-1}$ found here.

## DISCUSSION

Two main features arise from the combined study of the chimeric RC by either equilibrium redox titration or kinetic analysis. Whereas the physico-chemical properties of the hemes embedded in the cytochrome subunit are remarkably conserved with respect to the parent species *B. viridis*, the $E_m$ of the $P^+/P$ couple is downshifted in the chimeric RC. Further, an electrostatic interaction of 50 mV raises the $E_m$ of the $P^+/P$ couple when the $c_{559}$ is oxidized. Although the situation where this interaction can be directly observed, as in the present case, by the deviation to a one-electron Nernst curve is singular, we wish to argue that electrostatic interactions between nearby redox centers are likely to be found as well in other multi-redox cofactor membrane proteins. Among these membrane proteins, the "parent" RCs of the chimera should be first considered. Interestingly, the redox titration of the $P^+/P$ couple in WT *R. gelatinosus* also displayed a significant deviation to a $n = 1$ Nernst curve. As discussed above, the deviation can be accounted for by an electrostatic interaction of 50 mV between P and the closest high potential heme. Further, it is noteworthy that the less pronounced deviation in the WT *R. gelatinosus* with respect to the chimeric RC is not an indication of a smaller electrostatic interaction. Indeed, according to Equation 12, a similar electrostatic interaction between two redox centers having $E_m$s differing by more than about 50 mV is not witnessed by a pronounced deviation to a one electron Nernst curve. This point is illustrated by the disappearance of the deviation to a one-electron Nernst curve and a higher apparent $E_m$ for P in the R264L mutant of the VC-F RC where the $E_m$ of the closest heme to P has been downshifted. With the $E_m$ of the $c_{559}$ heme being lower in the R264L mutant than in the native VC-F, the redox changes of P occur in a potential range where the closest heme is fully oxidized. As a consequence, the electrostatic interaction between these two redox centers contributes to upshift the apparent $E_m$ of P when compared with the native VC-F RC. In *B. viridis*, the resolution of the three-dimensional structure (9) and the determination of the order of the hemes in the cytochrome subunit (24, 27, 28) grounded several studies that emphasized the role of intercofactor electrostatic interaction. Based on the finding that the oxidation of the outermost solvent-exposed hemes was moderately electrogenic, Gao *et al.* (29) estimated the interaction between $P^+$ and the $c_{559}$ heme in *B. viridis* to be 30 mV (29), in qualitative

agreement with our finding. When their three-dimensional structure is known, proteins are liable to electrostatic calculation. The Poisson-Boltzmann equation may be solved numerically and yield electrostatic interaction between cofactors (for example, see Refs. 1, 30, and 31). Gunner and Hönig (7) performed such calculations with the *B. viridis* RC and calculated, for the four hemes, the shifts in $E_m$s relative to solution (7). Electrostatic interactions among the four hemes of the tetraheme subunit ranged from 5 to 77 mV (7). The $P^+$/P couple was not treated in this study, probably because of the lack of reliable redox titration of this cofactor in solution due to its peculiar dimeric character. Yet, based on a kinetic analysis of the reduction of $P^+$ by the $c_{559}$ in whole cells, Baymann and Rappaport (13) conclude that the equilibrium constant of this reaction was significantly lower than predicted from the difference in $E_m$ of the two couples. The rationale for this apparent discrepancy was proposed to be an electrostatic interaction of 80 mV between these two cofactors (13).

As an example pertaining to respiratory chains, the succinate quinol reductase binds three iron sulfur clusters, which are thought to act as the entry path for electron. Interestingly, as determined by redox titration, the second cluster in the chain has a remarkably low redox potential (−250 mV) when compared with those of its two neighbors (−25 and −60 mV) (32). If this $E_m$ corresponds to the operating potential of this cofactor, it would make its reduction highly endergonic (for review see Ref. 33). Although, an energetically uphill step in an overall exergonic chain is not to be excluded *per se*, it has been proposed that this highly reducing $E_m$ reflects an anti-cooperative electrostatic interaction among redox centers rather than the "true operating" midpoint potential of this singular cluster (34).

The suggestion reported here that the $E_m$ of a redox cofactor depends on the redox state of its neighboring redox cofactor raises the question of the dielectric properties of the protein medium. This question has been extensively studied, and the emerging picture is that the screening of the electrostatic interaction between charges is best described by an effective distance-dependent dielectric constant. This phenomenological description was detailed by Schutz and Warshel (35) and experimentally supported by various groups (for review see Ref. 36 for the *Rhodobacter sphaeroides* reaction center case and references therein). By studying the shift in $E_m$ of the $P^+$/P couple in *R. sphaeroides* reaction center induced by mutations of ionizable groups at selected sites, Johnson and Parson (36) conclude that, although proteins are usually thought as a low dielectric medium, electrostatic interactions resulting from a change in the charge distribution around P are efficiently screened with an average screening factor of ~40 (36). With an electrostatic interaction of 50 mV between P and its closest heme located at 20 Å (center to center), we get by applying the Coulomb's law an average screening factor of 16, which is significantly larger than the value of 2–4 often used in electrostatic calculations but yet significantly lower than the value found by Johnson and Parson (36), suggesting that the screening of buried charges is less efficient in the present case than in their work. The various reasons, which may concur to this smaller screening factor, are as follows: (i) the fact that we are dealing here with electrostatic interaction between redox cofactors and not between ionizable side chains and a redox cofactor; (ii) the probable larger shielding from the bulk resulting from the binding of the cytochrome subunit to the RC in the present case at variance with the *R. sphaeroides* RC; and/or (iii) the preservation of the membrane environment in the present study. In line with this finding, Maki *et al.* (14) measured the redox potential of the $c_{559}$ heme in RC from the VC-F strain either embedded in their native membrane or solubilized in detergent and found a lower value in the case of solubilized reaction centers than with membrane fragments (14).

Obviously, the question of electrostatic interaction between cofactors should not be restricted to photosynthetic RC's. In order to achieve electron transfer reactions with rates compatible with biological catalysis, the electron donor and acceptor are usually located within 15 Å apart (37), an edge-to-edge distance similar to the one between P and the closest high-potential heme, here. This principle is likely to apply to all the membrane bound proteins involved in bioenergetic processes.

*Acknowledgments*—We thank W. Nitschke and B. Schoepp-Cothenet for EPR facilities. J. Lavergne and L. Baciou are warmly acknowledged for fruitful, critical, and stimulating discussions.

REFERENCES

1. Gunner, M. R., Alexov, E., Torres, E., and Lipovaca, S. (1997) *J. Biol. Inorg. Chem.* **2,** 126–134
2. Parson, W. W., Chu, Z.-T., and Warshel, A. (1990) *Biochim. Biophys. Acta* **1017,** 251–272
3. Warshel, A., and Aqvist, J. (1991) *Annu. Rev. Biophys. Biophys. Chem.* **20,** 267–298
4. Armstrong, F. A., Camba, R., Heering, H. A., Hirst, J., Jeuken, L. J., Jones, A. K., Leger, C., and McEvoy, J. P. (2000) *Faraday Discuss. Chem. Soc.* **116,** 191–203
5. Woodbury, N. W., Parson, W. W., Gunner, M. R., Prince, R. C., and Dutton, P. L. (1986) *Biochim. Biophys. Acta* **851,** 6–22
6. Sebban, P., and Wraight, C. A. (1989) *Biochim. Biophys. Acta* **974,** 54–65
7. Gunner, M. R., and Honig, B. (1991) *Proc. Natl. Acad. Sci. U. S. A.* **88,** 9151–9155
8. Nitschke, W., and Rutherford, A. W. (1994) *Biochem. Soc. Trans.* **22,** 694–699
9. Deisenhofer, J., Epp, O., Miki, K., Huber, R., and Michel, H. (1985) *Nature* **318,** 618–624
10. Nitschke, W., and Dracheva, S. M. (1995) in *Anoxygenic Photosynthetic Bacteria* (Blankenship, R. E., Madigan, M. T., and Bauer, C. E., eds) pp. 775–805, Kluwer Academic Publishers, Dordrecht, The Netherlands
11. Ortega, J. M., and Mathis, P. (1993) *Biochemistry* **32,** 1141–1151
12. Ortega, J. M., and Mathis, P. (1992) *Photosynth. Res.* **34,** 127–127
13. Baymann, F., and Rappaport, F. (1998) *Biochemistry* **37,** 15320–15326
14. Maki, H., Matsuura, K., Shimada, K., and Nagashima, K. V. P. (2003) *J. Biol. Chem.* **278,** 3921–3928
15. Nagashima, K. V. P., Shimada, K., and Matsuura, K. (1996) *FEBS Lett.* **385,** 209–213
16. Nagashima, K. V. P., Matsuura, K., Shimada, K., and Verméglio, A. (2002) *Biochemistry* **41,** 14028–14032
17. Nagashima, K. V. P., Alric, J., Matsuura, K., Shimada, K., and Verméglio, A. (2004) *13th International Congress on Photosynthesis* (Bruce, D., and van der Est, A., eds) Allen Press, Montréal
18. Rutherford, A. W., and Sétif, P. (1990) *Biochim. Biophys. Acta* **1019,** 128–132
19. Baymann, F., Moss, D. A., and Mantele, W. (1991) *Anal. Biochem.* **199,** 269–274
20. Joliot, P., Béal, D., and Frilley, B. (1980) *J. Chim. Phys.* **77,** 209–216
21. Béal, D., Rappaport, F., and Joliot, P. (1999) *Rev. Sci. Instrum.* **70,** 202–207
22. Dutton, P. L. (1971) *Biochim. Biophys. Acta* **226,** 63–80
23. Agalidis, I., and Sebban, P. (1995) *Biochim. Biophys. Acta* **1232,** 180–186
24. Nitschke, W., and Rutherford, A. W. (1989) *Biochemistry* **28,** 3161–3168
25. Dracheva, S. M., Drachev, L. A., Zaberezhnaya, S. M., Konstantinov, A. A., Semenov, A. Y., and Skulachev, V. P. (1986) *FEBS Lett.* **205,** 41–46
26. Chen, I. P., Mathis, P., Koepke, J., and Michel, H. (2000) *Biochemistry* **39,** 3592–3602
27. Verméglio, A., Richaud, P., and Breton, J. (1989) *FEBS Lett.* **243,** 259–263
28. Alegria, G., and Dutton, P. L. (1991) *Biochim. Biophys. Acta* **1057,** 258–1972
29. Gao, J.-L., Shopes, R. J., and Wraight, C. A. (1990) *Biochim. Biophys. Acta* **1015,** 96–108
30. Ullmann, G. M., and Knapp, E. W. (1999) *Eur. Biophys. J.* **28,** 533–551
31. Warshel, A., and Papazyan, A. (1998) *Curr. Opin. Struct. Biol.* **8,** 211–217
32. Unden, G., Hackenberg, H., and Kroger, A. (1980) *Biochim. Biophys. Acta* **591,** 275–288
33. Hagerhall, C. (1997) *Biochim. Biophys. Acta* **1320,** 107–141
34. Salerno, J. C. (1991) *Biochem. Soc. Trans.* **19,** 599–605
35. Schutz, C. N., and Warshel, A. (2001) *Proteins* **44,** 400–417
36. Johnson, E. T., and Parson, W. W. (2002) *Biochemistry* **41,** 6483–6494
37. Page, C. C., Moser, C. C., Chen, X., and Dutton, P. L. (1999) *Nature* **402,** 47–52
38. Rappaport, F., Béal, D., Verméglio, A., and Joliot, P. (1998) *Photosynth. Res.* **55,** 317–323